A Study of Transient Liquid-Phase Bonding of Ag-Cu Using Differential Scanning Calorimetry

M.L. KUNTZ, Y. ZHOU, and S.F. CORBIN

A novel approach using differential scanning calorimetry (DSC) to quantify interface kinetics in a solid/liquid diffusion couple is applied to characterize the isothermal solidification stage during transient liquid-phase (TLP) bonding of Ag and Cu using a Ag-Cu interlayer. When the DSC results are properly interpreted, the measured interface kinetics are more accurate than those obtained using traditional metallographic techniques. Experimental results are compared to predictions for isothermal solidification given by a selection of analytical models. The comparison yields close agreement with a solution that assumes a moving boundary; but accuracy of the predictions is very sensitive to selection of solute diffusivity. Metallographic inspection of the DSC samples and traditional TLP bonds validates the kinetics measured using this technique, and supports the prediction given by the analytical model. This study shows that the method of using DSC to quantify interface kinetics is valuable in the refinement of process parameters for TLP bonding. Furthermore, simple analytical solutions can be applied to predict the process kinetics of isothermal solidification in simple binary systems with considerable accuracy when the effects of grain boundaries can be neglected, thus reducing the need for complex numerical models when developing process parameters.

I. INTRODUCTION

TRANSIENT liquid-phase (TLP) bonding[1] is a material joining process that produces a high quality bond at the interface of the parts to be joined.[2] The TLP bonding, which is also known as diffusion brazing,[3] is a brazing or soldering variation; and, as such, it depends on the formation of a liquid at the faying surfaces by an interlayer that melts at a temperature lower than that of the substrate. The TLP bonding is distinguished from other brazing processes by the resolidification of this liquid at a constant temperature. The interlayer is rich in a melting point depressant, and upon heating through the eutectic temperature, the interlayer will either melt or react with the base metal to form a liquid. During an isothermal hold above the melting temperature of the interlayer, the melting point depressant (solute) is removed from the liquid phase through extensive long-range diffusion into the base metal (solvent). The resulting solid/liquid interfacial motion via epitaxial growth of the substrate is termed ''isothermal solidification.''[2] A homogeneous bond between the substrates is formed when isothermal solidification is complete, which is when the two solid/liquid interfaces meet at the joint centerline.

The TLP bonding shows great potential for joining materials that are not easily joined by conventional fusion welding processes.[4–8] One reason that TLP bonding is not yet in widespread use is that the experimental approach used to determine the process parameters can be time consuming and costly. This experimental approach typically involves a determination of the liquid fraction remaining in the joint metallographically from a series of samples quenched from the process temperature at different hold times.[9] The width of a solidified liquid phase is identified by a eutectic microstructure and measured from a cross section of the joint. Unfortunately, the solid/liquid interface is usually not planar but irregular and scalloped, which makes measurement of the eutectic width difficult and prone to measurement error.[10] In some studies of isothermal solidification kinetics, the eutectic width is assumed to be representative of the liquid width before cooling.[11–15] Nakao *et al.*[16] and MacDonald and Eagar[10] used the lever rule to account for primary solidification, which has been shown to occur epitaxially during cooling.[17] Both of these methods assume ideal conditions that are unlikely during solidification. MacDonald and Eagar[18] have explained that experimental setup can also be a source of significant error. The apparent overall isothermal solidification time can be reduced by the squeezing of liquid from the interface due to excessive force in the assembly. Liquid can also be lost from the joint area through wetting of the sides of the base metal. Furthermore, fixing the base metal samples at a set distance does not accommodate volumetric changes and can result in porosity. It is difficult to experimentally measure interface kinetics accurately using metallographic techniques.

Recently, differential scanning calorimetry (DSC) has been used to accurately quantify the kinetics of interface motion in a solid/liquid diffusion couple.[19] This can be applied to TLP bonding in binary alloy systems to characterize the kinetics of isothermal solidification. In previous relevant work, Corbin and Lucier[20] have successfully used the DSC to measure process kinetics of the TLP sintering process; however, it has been shown that geometrical differences in the TLP bonding process profoundly affect the DSC results and this requires additional interpretation.[19] Venkatraman *et al.*[21] studied the kinetics of low-temperature TLP solidification in electroplated Au-Sn layers on Cu using DSC, but the thin width of the base metal in their study does not support the semi-infinite thickness assumption made in the analytical models. Their work also shows a systematic underestimation of the fraction of liquid remaining after an isothermal hold period.[22] Recent efforts have shown that this effect is a result of the planar nature of the

M.L. KUNTZ, Research Assistant, Y. ZHOU, Associate Professor and Canada Research Chair, and S.F. CORBIN, Associate Professor, are with the Department of Mechanical Engineering, University of Waterloo, Waterloo, ON, Canada, N2L 3G1. Contact e-mail: mlkuntz@uwaterloo.ca

Manuscript submitted December 2, 2005.

solid/liquid interface and can be corrected with the appropriate measures.[19]

The advantage of using DSC is that it greatly reduces the operator error in the measurement system. The variation in liquid width across the interface that results in measurement error using traditional techniques is insignificant when using the DSC. In addition, the DSC can quantitatively measure the liquid fraction present over the entire bond area. The DSC method is a cost-effective and reliable alternative for easily developing TLP bonding process parameters. The objectives of this work are to apply the DSC method for measuring solid/liquid interface kinetics to the isothermal solidification stage during TLP bonding. The results can then be compared to the predictions for completion of isothermal solidification given by a selection of analytical models. Finally, metallographic techniques will be used to verify the accuracy of the DSC results and model predictions.

II. PROCESS DESCRIPTION

A comprehensive description of the TLP bonding process is given in the review article by Zhou *et al.*[2] The four discrete stages of the TLP bonding process are (1) heating, (2) dissolution and widening, (3) isothermal solidification, and (4) homogenization.[2,18,23] MacDonald and Eagar describe two process variants: the type-I process, which employs a pure interlayer; and the type-II process, which employs an interlayer near the liquidus composition at the bonding temperature.[7] A theoretical description of the process assuming a eutectic interlayer (type II) is given here, and the process is similar for any interlayer composition. Initially, two base metal substrates with composition C_0 are brought into intimate contact with an interlayer of composition C_F placed at the faying surfaces. The initial width of the interlayer is W_0, and the width of the substrate is assumed infinite.

During the heating stage, the entire assembly is heated from room temperature to just below the eutectic. Solid-state diffusion between the interlayer and the base metal occurs, resulting in the composition profile shown by the schematic in Figure 1.

When the eutectic temperature is reached, the interlayer melts and wets the substrate. As the temperature is increased past the eutectic, the compositions of the solid and liquid at the solid/liquid interface, C_S and C_L, respectively, track along the phase boundaries, as predicted by the phase diagram. As the base metal is dissolved, the liquid zone widens to maintain the mass balance given in Eq. [1], where the *X(t)* is the position of the solid/liquid interface, and D_S and D_L are the solute diffusivities in the solid and liquid, respectively. The dissolution stage, shown schematically in Figure 2, is complete when the maximum liquid width (W_{max})[2] is reached and the composition of the liquid is uniform;[24] this depends on interface kinetics and does not necessarily coincide with the time when the bonding temperature (T_b) is attained.

$$(C_L - C_S) \cdot \frac{d}{dt} X(t) = D_S \cdot \frac{\partial}{\partial x} C_S - D_L \cdot \frac{\partial}{\partial x} C_L \qquad [1]$$

At the bonding temperature, diffusion of the melting point depressant solute across the solid/liquid interface into the base metal occurs. To maintain equilibrium, as predicted by

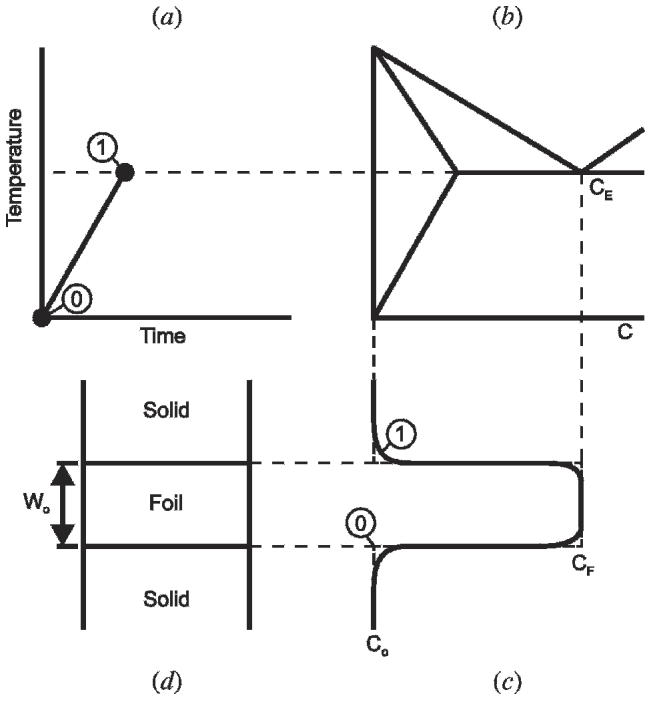

Fig. 1—Heating stage (*a*) thermal profile, (*b*) phase diagram, (*c*) composition profile, and (*d*) bond schematic. Point 0: initial conditions; Point 1: end of stage 1; Point 2: end of stage 2.

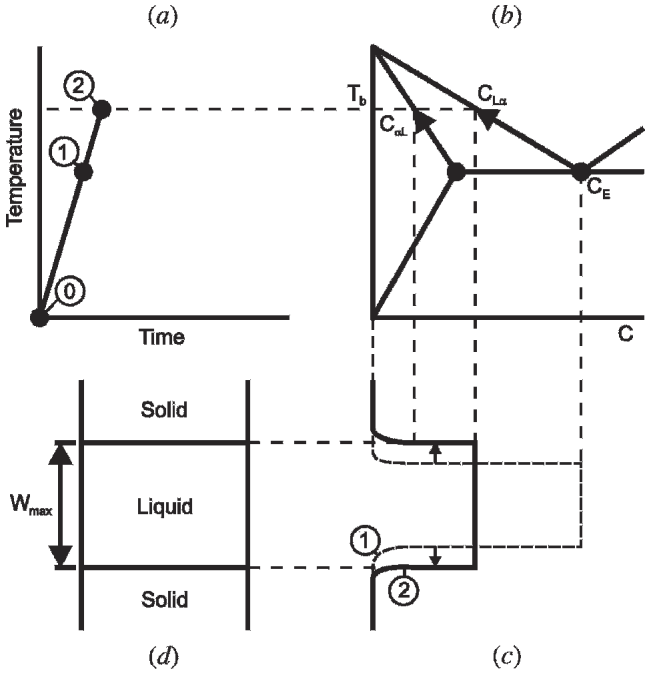

Fig. 2—Dissolution and widening stage: (*a*) thermal profile, (*b*) phase diagram, (*c*) composition profile, and (*d*) bond schematic. Point 0: initial conditions; Point 1: end of stage 1; Point 2: end of stage 2.

the phase diagram, the liquid composition is constant at $C_{L\alpha}$. The width of the liquid zone must decrease to satisfy the mass balance (Eq. [1]) as the solute is lost. This process of solid/liquid interface motion toward the joint centerline, as shown in Figure 3, is termed isothermal solidification.[2]

When the two solid/liquid interfaces meet at the end of isothermal solidification, a solute peak with the composition

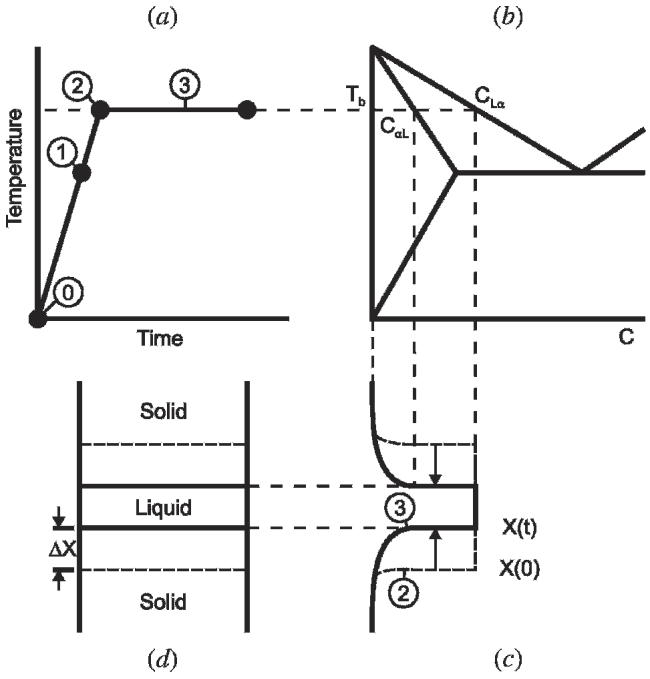

Fig. 3—Isothermal solidification stage: (*a*) thermal profile, (*b*) phase diagram, (*c*) composition profile, and (*d*) bond schematic. Point 0: initial conditions; Point 1: end of stage 1; Point 2: end of stage 2; Point 3: some time during stage 3.

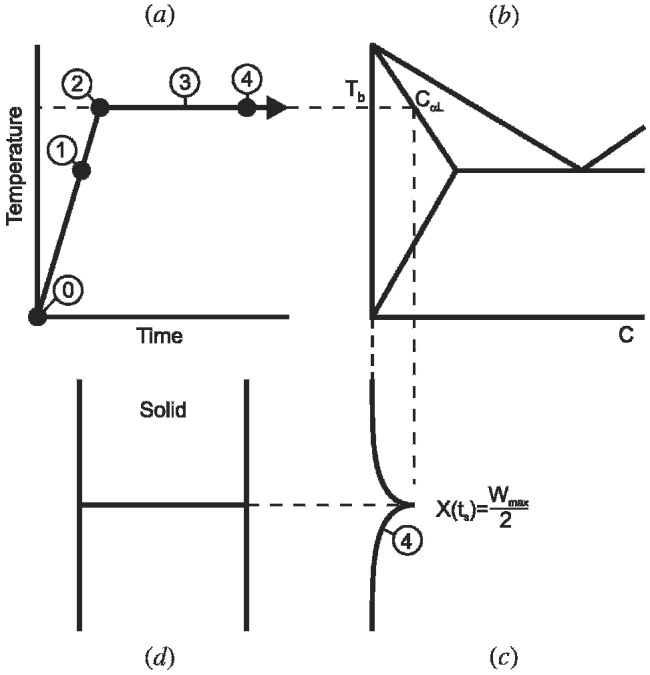

Fig. 4—Homogenization stage: (*a*) thermal profile, (*b*) phase diagram, (*c*) composition profile, and (*d*) bond schematic. Point 0: initial conditions; Point 1: end of stage 1; Point 2: end of stage 2; Point 3: some time during stage 3; Point 4: end of stage 3.

$C_{\alpha L}$ will remain at the joint centerline, as detailed in Figure 4. Through solid-state diffusion at an elevated temperature, the composition of the final solute peak is gradually decreased over time until an acceptable solute level is reached.

The two most important stages in terms of joint quality are the isothermal solidification and the homogenization stages; coincidently, it is also these stages that require the longest time for completion since they are controlled by solute diffusion in the solid.[25] In systems with a low solubility limit, the isothermal solidification stage becomes longer. Conversely, in some systems with a high solubility limit, the homogenization stage requires longer time for completion. It is essential that each stage is not terminated before completion, or the resulting heterogeneous microstructure (caused by solute rejection or precipitation) will degrade mechanical properties.[1] Thus, it is highly desirable to have an accurate measure of the process kinetics of the isothermal solidification stage when setting process parameters in order to prevent premature cooling while minimizing process time.

III. EXPERIMENTAL METHODS

In the current study, pure Ag and pure Cu were selected for the solid phase (base metal) with Ag-Cu interlayer alloys. The binary equilibrium-phase diagram shows the system is a simple binary with a eutectic at 780 °C and 28 wt pct Cu, and that no stable intermetallics will form.[26] Furthermore, Ag can be considered inert at the process temperature; thus, the formation of contaminants (*e.g.,* mainly oxides), which could inhibit isothermal solidification, is not expected to be significant on the surface of the solid. Tuah-Poku *et al.*[27] and MacDonald and Eagar[10] have performed relevant work on TLP bonding in the Ag-Cu binary system; thus, the results of this study can be compared to those in the literature.

A. *DSC Setup*

Base metal right cylinders with a diameter of 5 mm and a 3-mm thickness were prepared from 99.95 pct pure Ag and Cu rod from Alfa Aesar (Ward Hill, MA). The faying surface was ground flat with 1200 grit paper and cleaned ultrasonically with acetone before joining. Three interlayer compositions were studied, the Ag-Cu eutectic (Ag-28 wt pct Cu), Ag-24 wt pct Cu, and Ag-10 wt pct Cu. The eutectic foil was obtained from Lucas Milhaupt (99.9 pct pure). The 24 pct Cu and 10 pct Cu foils were not commercially available and were fabricated by casting from high-purity powders (Alfa Aesar). The cast ingot was then rolled to a thin foil in a series of steps, each step followed by a recovery anneal. The nominal interlayer thickness was 25.4 μm, and it was cleaned ultrasonically with acetone before joining.

The side of the cylinder was coated with an alumina lubricant to prevent the liquid from wetting any surface of the cylinder other than the faying surface. A TLP ''half-sample'' consisting of the base metal and Ag-Cu interlayer was placed in an alumina DSC sample crucible. The TLP half-samples consist of one half of the assembly divided by the joint centerline. These samples were used to simulate the TLP bonding process so that the area of interest, the liquid zone, was nearest the measuring thermocouples. Since the TLP bond is symmetrical, using a half-sample will have no effect on the kinetics of the process with the exception of possible surface evaporation of the Cu solute. This was considered by MacDonald and Eagar,[10] who pointed out that solute loss due to vaporization could be estimated using Langmuir's equation. Since the partial equilibrium vapor pressure of Cu is negligible at the isothermal hold temperature, the effect of vaporization is expected to be minimal

and can be assumed zero. Specific information regarding the DSC experimental setup is given in the account of previous work.[19]

A dynamic nitrogen atmosphere was used in the DSC for all trials. The initial heating rate was 40 °C/min. At 700 °C, the heating rate was reduced to 10 °C/min for enhanced measurement resolution and reduced thermal lag in the temperature range of interest. The bonding temperature was 800 °C. The isothermal hold time at the bonding temperature was varied from zero to the time required for isothermal solidification to near completion. The cooling cycle was opposite the heating cycle.

The DSC measures heat flow of the sample relative to a reference cell during heating or cooling. Heat flow is measured using a pair of thermocouples that compare the temperature change of reference and sample cells. Thus, the DSC is capable of studying the kinetics of thermal events, such as phase changes. Experimental results are given in the form of a DSC trace, which shows the heat flow of a thermal event as either endothermic or exothermic peaks (*i.e.*, melting or solidification, respectively). The integral of the peak is a measure of the enthalpy of the event, and when an isothermal hold time is inserted between the heating and cooling of a TLP-bonded sample, a ratio of the exotherm to the endotherm is an indication of the amount of liquid remaining, which traditionally has been found using metallographic examination.

The heating and cooling segments at 10 °C/min, which pass through the melting temperature of the Ag-Cu eutectic foil (*i.e.*, 780 °C), are the segments used to quantify isothermal solidification. This portion of the DSC trace is plotted in Figure 5 as a function of heat flow *vs* temperature. Integration of the melting or solidification peaks gives the total energy of the thermal event. Since the composition of the liquid is constant throughout the isothermal solidification stage, the heat of formation of the liquid, Δh_f will remain unchanged. Thus, the ratio of the solidification endotherm, ΔH_s, to the melting exotherm, ΔH_f, will be the amount of liquid remaining at the termination of the isothermal hold period (Eq. [2]).

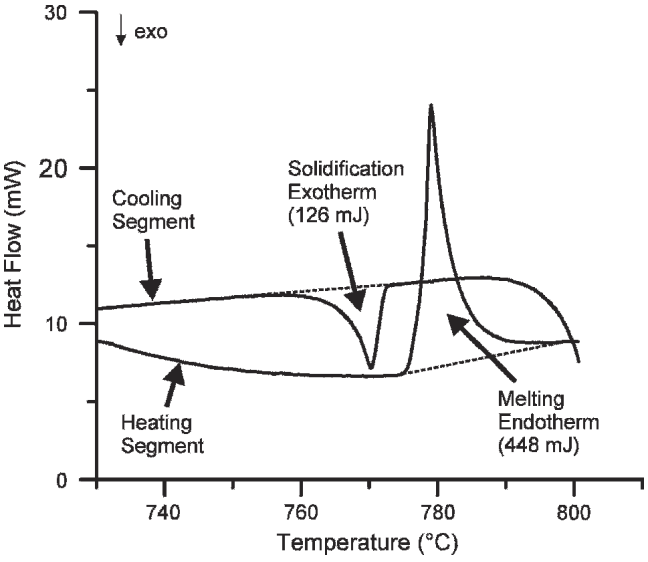

Fig. 5—Melting and solidification peaks on DSC trace of TLP half-sample.

$$\text{fraction of liquid remaining} = \psi \frac{\Delta H_s}{\Delta H_f} \qquad [2]$$

where the constant, ψ, is experimentally determined for the system.[19]

The correction is required due to a systematic underestimation of the residual liquid in the results that is related to the effects of the TLP half-sample geometry. First, baseline shift on the DSC trace during initial dissolution of the foil increases the measured enthalpy of melting.[19] The thermal contact resistance at the interlayer/base-metal interface is reduced as liquid wets the faying surface, which causes a shift in the baseline across the endothermic melting peak. Second, epitaxial solidification of a primary phase at the solid/liquid interface upon cooling from the bonding temperature to the eutectic temperature reduces the measured enthalpy of solidification.[19] The exothermic solidification peak includes only the enthalpy of eutectic solidification; primary epitaxial growth of the solid phase is not measured in this arrangement. These effects can be quantified using a modified temperature program and are constant as isothermal solidification progresses. The effects of baseline shift and primary solidification are included in the experimentally derived constant (Ψ), which is multiplied with the enthalpy ratio to accurately represent the fraction of liquid remaining.

The interface position (Eq. [3]) can be calculated from the fraction of liquid remaining (Eq. [2]) using the theoretical maximum liquid width, given by Eq. [4].

$$X(t) = \left(1 - \psi \frac{\Delta H_s}{\Delta H_f}\right) \cdot \frac{W_{\max}}{2} \qquad [3]$$

$$W_{\max} = \frac{C_F \cdot W_0}{C_{L\alpha}} \qquad [4]$$

B. *Metallurgical Examination*

The DSC half-samples were sectioned and mounted in a bakelite resin. The samples were polished to 1 μm using a diamond suspension. The samples were then etched using a 20 mL NH_4OH, 20 mL H_2O_2, and 10 mL H_2O solution. The solid/liquid interface region was inspected using optical and scanning electron microscopy. A composition profile of the Cu in the Ag base metal was obtained using a spot EDS analysis at measured intervals from the solid/liquid interface.

IV. RESULTS AND DISCUSSION

A. *Analytical Models for Isothermal Solidification*

The experimental results are compared to analytical predictions for solid/liquid interface motion. Two models are taken from the literature, while a third is derived subsequently. The models can give widely varying results depending on process conditions. Tuah-Poku *et al.*[27] suggested that the kinetics predicted by analytical models do not agree well with the experimental observations. For the derivation of the analytical models, the review article by Zhou *et al.*

should be referenced.[2] In this study, the isothermal solidification stage is treated as a discrete stage in the TLP bonding process. The following assumptions are made in the derivation: no solute is lost to the base metal before the isothermal solidification stage begins; solute distribution in the liquid is uniform throughout the stage;[24] the solid/liquid interface is at equilibrium; the solid/liquid interface movement is planar; and the base metal substrate width is semi-infinite when compared to the interlayer width.

A simple solution for the total time required for isothermal solidification (t_s) can be found by assuming a solute composition profile based on a stationary solid/liquid interface. The isothermal solidification time is found by equating the total solute content in the liquid to the interface flux integrated over the isothermal hold period. The solution is given by Eq. [5].[27]

$$t_s = \frac{\pi}{16 \cdot D_s} \cdot \left(\frac{C_F \cdot W_0}{C_{\alpha L} - C_0} \right)^2 \qquad [5]$$

The composition solution is based on the assumption that the solid/liquid interface is stationary with respect to the base metal. A more rigorous treatment of the problem treats the solid/liquid interface as a moving boundary. Ikawa *et al.*[9] present a solution for the moving interface problem by assuming that the concentration profile of the solute in the base metal has the same form as the stationary case, except with a shifting reference frame that is fixed to the solid/liquid interface. The position of the solid/liquid interface is given by Eq. [6].[16]

$$X(t) = \frac{C_0 - C_{\alpha L}}{C_{L\alpha} - C_{\alpha L}} \cdot 2 \cdot \sqrt{\frac{D_s \cdot t}{\pi}} \qquad [6]$$

The time required for completion of isothermal solidification can be found when the solid/liquid interface reaches the joint centerline, given by Eq. [7].

$$t_s = \frac{\pi}{16 \cdot D_s} \cdot \left(\frac{C_F \cdot W_0}{C_{L\alpha}} \cdot \frac{C_{L\alpha} - C_{\alpha L}}{C_0 - C_{\alpha L}} \right)^2 \qquad [7]$$

The result (Eq. [7]) is very similar to the solution for a stationary interface (Eq. [5]); and, although there is an assumption of a moving boundary, it does not account for the sweeping action of the solid/liquid interface as it advances toward the centerline. A theoretically accurate account of the moving interface was first given by Lesoult.[28] A similar solution derived subsequently follows the work of Maugis *et al.*[29] on biphase diffusion couples. This solution was first applied to TLP bonding by Sinclair[30] in work on multicomponent systems. A substitution variable, λ, given by Eq. [8] is substituted into Fick's second law to yield Eq. [9].

$$\lambda = \frac{x}{\sqrt{t}} \qquad [8]$$

$$-\frac{\lambda}{2} \cdot \frac{dC}{d\lambda} = D \cdot \frac{d^2C}{d\lambda^2} \qquad [9]$$

The boundary condition on Eq. [9] is $C(\xi) = C_{\alpha L}$, where the rate constant, ξ, is defined by the interface (*i.e.*, $\lambda_i = \xi$). It can be easily shown that Eq. [10] is a solution of the ordinary differential equation.

$$C(\lambda) = C_{\alpha L} \cdot \frac{\operatorname{erfc}\left(\frac{\lambda}{2 \cdot \sqrt{D}} \right)}{\operatorname{erfc}\left(\frac{\xi}{2 \cdot \sqrt{D}} \right)} \qquad [10]$$

The position of the solid/liquid interface, *X(t)* can then be written by Eq. [11]. The parabolic nature of the interface position is not an assumption, but rather a property of the exact solution.

$$X(t) = \xi \cdot \sqrt{t} \qquad [11]$$

The mass balance given by Eq. [12] can be used to find the interface rate constant, ξ, and the time required for completion of the isothermal solidification stage, where k is a partition coefficient given by $C_{L\alpha}/C_{\alpha L}$. Equation [13] must be solved numerically to find the constant, ξ.

$$C_{\alpha L} \cdot (k-1) \cdot \frac{\xi}{2\sqrt{t}} = D \cdot \frac{dC}{d\lambda}_{\lambda = \xi} \cdot \frac{1}{\sqrt{t}} \qquad [12]$$

$$\xi = -2(k-1)^{-1} \cdot \sqrt{\frac{D}{\pi}} \cdot \frac{\exp\left(\frac{-\xi^2}{4 \cdot D} \right)}{\operatorname{erfc}\left(\frac{\xi}{2\sqrt{D}} \right)} \qquad [13]$$

The significance of the interface rate constant, ξ, is that it is an indication of the isothermal solidification rate. Increasing ξ results in faster solid/liquid interface motion and shorter duration of the isothermal solidification stage. Furthermore, ξ is independent of the initial liquid width; thus, it is useful to discuss process kinetics in terms of ξ rather than the time required for isothermal solidification when the temperature and initial liquid width are varied.

The isothermal solidification stage is complete when the solid/liquid interface reaches the joint centerline; the time required is given by Eq. [14].

$$t_s = \left(\frac{-W_{\max}}{2 \cdot \xi} \right)^2 \qquad [14]$$

It is interesting to note that this solution gives the same result as a similar method derived by Danckwerts[31] and used by Lesoult,[28] which is described in detail by Zhou *et al.*[2] It is thought that the solution presented here is somewhat simpler in derivation.

B. *Predicted and Experimentally Measured Interface Kinetics*

The results of the DSC diffusion couple experiment for the Ag base metal with the eutectic interlayer held at 800 °C are given in Figure 6. As expected, the fraction of

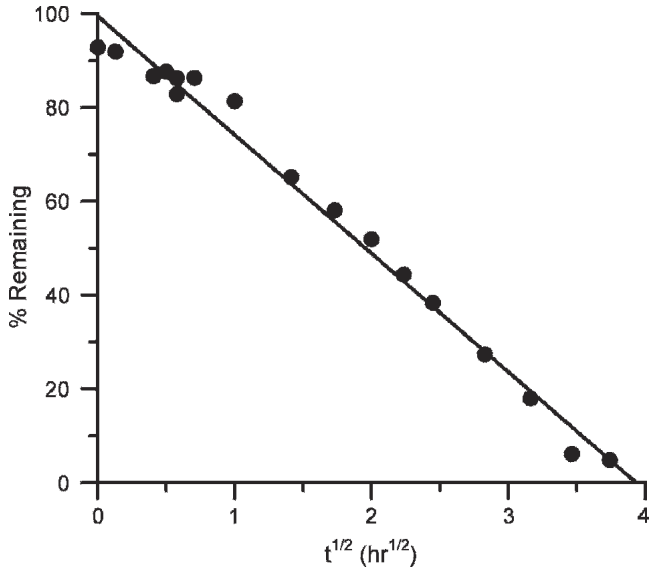

Fig. 6—Fraction of liquid remaining in TLP half-sample after isothermal hold time. The Ag base metal with 25-μm-thick eutectic Ag-Cu interlayer bonded at 800 °C.

liquid remaining is linearly proportional to the square root of the isothermal hold time. The experimental interface rate constant (ξ') can be found by combining Eq. [3] with Eq. [7], which results in Eq. [15]. The results in Figure 6 can be extrapolated to give the time for completion of isothermal solidification, which is when the liquid remaining is zero, or 15.5 hours. This gives a measured interface rate constant of $\xi' = -0.126\ \mu\text{m}/\sqrt{\text{s}}$, based on an initial liquid width ($W_{\max}$) of 59.5 μm (Eq. [4]).

$$\xi' = \frac{W_{\max}}{2 \cdot \sqrt{t_s}} \qquad [15]$$

The isothermal solidification kinetics generated from the DSC results can be compared to the predictions of the analytical models using the time for completion of isothermal solidification and the interface rate constant. At 800 °C, $C_{\alpha L}$ is 12.6 at. pct (7.8 wt pct) and $C_{L\alpha}$ is 34.9 at. pct (24 wt pct). Selection of an appropriate diffusion coefficient is difficult because published chemical diffusion data in the range of composition is unavailable. The diffusivity in Ag with a range of 0 to 2 at. pct Cu at 800 °C is reported to be 5.9×10^{-10} cm^2/s.[32] Homogeneous diffusion data show that diffusivity is enhanced with increasing concentration of Cu in Ag.[33] The published diffusion data for a 6.56 at. pct Cu homogeneous solution[33] gives a D_0 of 0.51 cm^2/s with an activation energy of 182.1 kJ/mol resulting in a diffusion coefficient of $D = 7.0 \times 10^{-10}$ cm^2/s at 800 °C. Taking the composition midpoint (*i.e.*, $C_{\alpha L}/2 + C_0/2 = 6.3$ pct), $D = 7.0 \times 10^{-10}$ cm^2/s can be considered a good "first approximation" in the absence of known diffusivity for these conditions.

Using this value, the predicted interface rate constant, ξ, is $-0.126\ \mu\text{m}/\sqrt{\text{s}}$ using Eq. [13]. This agrees exactly with the measured isothermal solidification kinetics, so the assumed diffusivity fits the results well. It should be noted that even though a constant D is assumed for model derivation, the diffusivity can vary significantly with C along the concentration profile. The assumed value will have a considerable effect on the simulation results; if a lower diffusivity value was selected, the interface kinetics would be slower. For example, if $D = 5.9 \times 10^{-10}$ cm^2/s, $\xi = -0.116\ \mu\text{m}/\sqrt{\text{s}}$, and the predicted isothermal solidification time would be 18.4 hours.

Using Eq. [5] for the stationary interface solution, isothermal solidification is predicted to require 21.3 hours. Zhou reported that the assumption of a stationary solid/liquid interface results in an overestimation that is largely dependant on $C_{L\alpha}$ and C_0.[34] Following the method developed by Zhou for the estimation error (Eq. [16]) derived from Eqs. [5] and [14] shows that the estimation error in the stationary solution gets large when C_0 or $C_{\alpha L}$ is large, or when $C_{L\alpha}$ gets relatively small.[34,35] In this study, the error associated with using the stationary interface is found to be 38 pct. These results show that the stationary solution can only be used under specific conditions if a minimal amount of estimation error is expected.

$$\text{Error} = \left[\frac{\pi \cdot \xi^2}{4D} \cdot \left(\frac{C_{L\alpha}}{C_{\alpha L} - C_0}\right)^2 - 1\right] \times 100\ \text{pct} \qquad [16]$$

Finally, the predicted isothermal solidification time using the shifting reference solution is 8.7 hours (Eq. [7]). This treatment; however, is not theoretically accurate since it assumes a stationary composition solution with a shifting reference frame and does not account for increased solute buildup in the base metal as a result of the sweeping action of the solid/liquid interface. The shape of the shifting reference profile is identical to that of the stationary interface profile with a shift from the original solid/liquid interface position.[35] This assumption virtually enhances flux at the solid/liquid interface and results in an overestimation of the isothermal solidification kinetics as shown in the results.

C. *Comparison of Results*

A summary of the experimental and modeling results is given in Table I. The interface kinetics can be compared in Figure 7, which shows the fraction of liquid remaining as measured by DSC with the predicted results. As shown, the best agreement is found with the moving interface solution ($\xi = -0.126\ \mu\text{m}/\sqrt{\text{s}}$). An equivalent interface rate constant for results given by the stationary solution as calculated using Eq. [15] is $\xi = -0.107\ \mu\text{m}/\sqrt{\text{s}}$. Similarly, the interface rate constant using the shifting reference solution is $\xi = -0.168\ \mu\text{m}/\sqrt{\text{s}}$. Examination of Figure 7 shows how the stationary solution underestimates the interface kinetics, while the shifting reference frame solution overestimates it.

As noted, the selected value for the solute diffusivity has a profound effect on the accuracy of the predicted isothermal solidification kinetics. An effective diffusivity, D_{eff}, can be found for each solution from the experimental results to give good agreement. For instance, $D_{\text{eff}} = 9.6 \times 10^{-10}$ cm^2/s is found using Eq. [5] (stationary), and similarly, $D_{\text{eff}} = 3.9 \times 10^{-10}$ cm^2/s is found using Eq. [7] (shifting reference). There is no preference for a particular model, except that the moving interface solution (Eq. [13]) is theoretically more accurate in its derivation. It is also this solution that

Table I. Summary of Experimental and Modeling Results for Ag-Base Metal Solid/Liquid Diffusion Couples (C_F = 28 Pct Cu, T_b = 800 °C, $D = 7.0 \times 10^{-10}$ cm²/s)

Calculation Method	ξ (μm/$\sqrt{s}$)	t_s (h)
Experimental DSC results	−0.126	15.5
Moving interface solution (Eqs. [13] and [14])	−0.126	15.5
Shifting reference solution (Eqs. [6] and [7])	−0.107	21.3
Stationary solution (Eq. [5])	−0.168	8.7

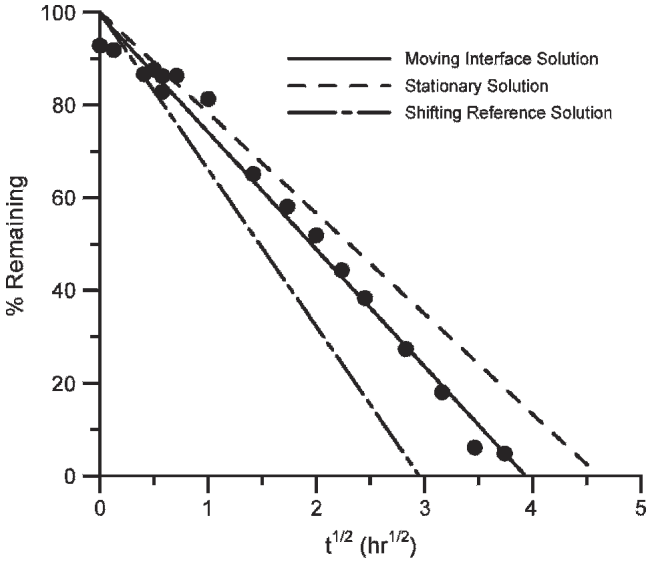

Fig. 7—Comparison of experimental results for Ag-Cu eutectic interlayer with analytical modeling predictions.

gives the closest agreement to experimental results using the published diffusion data.

The DSC results can also be compared to interface kinetics reported in the literature (Table II). Tuah-Poku *et al.*[27] measured isothermal solidification kinetics for TLP bonds at 820 °C with pure Ag-base metal and an 80-μm-thick pure Cu interlayer and reported excessive inaccuracy with the analytical models. From their experimental results, which were collected using visual inspection of metallurgically prepared samples, an interface rate constant, ξ', was found to be -0.290 μm/$\sqrt{s}$.[27] Since these experiments were conducted at a higher temperature than the DSC trials (820 °C *vs* 800 °C), the interface kinetics are expected to differ somewhat. If the diffusivity value used earlier is corrected for the increase in temperature, $D = 1.0 \times 10^{-9}$ cm²/s. With $C_{\alpha L} = 11.3$ at. pct (7.0 wt pct) and $C_{L\alpha} = 29.8$ at. pct (20 wt pct), the predicted interface rate constant is -0.160 μm/$\sqrt{s}$, which is significantly slower than the reported value. The difference between experimental and predicted results is likely due to a combination of experimental error and inaccuracy in the diffusion data. An effective diffusivity for the results can be found using Eq. [13], which gives a value of $D_{\text{eff}} = 3.3 \times 10^{-9}$ cm²/s.

Tuah-Poku *et al.* repeated their experiment using a 75-μm-thick Ag-20 wt pct Cu foil interlayer at the same bonding temperature.[27] Isothermal solidification was reported to be complete, except for some liquid trapped at the grain boundaries after 8 hours, for which $\xi' = -0.221$ μm/$\sqrt{s}$, which gives an effective diffusivity of $D_{\text{eff}} = 1.9 \times 10^{-9}$ cm²/s. There is a significant difference between the experimental results. Since T_b for both trials is the same, the isothermal solidification kinetics are expected to be similar, because the interface rate constant is unaffected by changes in interlayer thickness or composition. According to Tuah-Poku *et al.*, the nonplanar characteristics of the interface make it difficult to accurately make a quantitative measure of the isothermal solidification kinetics, because at some areas, liquid is trapped at the grain boundaries, while at others, isothermal solidification is complete. Using the predicted interface rate constant (-0.160 μm/$\sqrt{s}$), 27 pct of the liquid is expected to remain after 8 hours. Thus, the difference between the results of Tuah-Poku *et al.* is likely due to measurement and experimental error, such as squeezing of liquid from the joint. The DSC results, however, provide an accurate representation of the process kinetics because they are not prone to measurement error of this nature.

Table II. Comparison of Experimental Interface Kinetics Measured using DSC and Traditional Techniques for Ag-Base Metal

C_F	T_b (°C)	ξ (μm/$\sqrt{s}$)	D_{eff} (cm²/s)
DSC method			
28 pct Cu	800	−0.126	7.0×10^{-10}
24 pct Cu	800	−0.128	7.3×10^{-10}
10 pct Cu	800	−0.452	6.4×10^{-9}
Visual inspection[27]			
Cu	820	−0.290	3.3×10^{-9}
Cu	820	−0.221	1.9×10^{-9}

There is a marked difference between the results collected by Tuah-Poku *et al.*, using visual inspection, and the results collected using DSC under similar experimental conditions, even when the small difference in temperature is considered. In the current study, the DSC experiment was repeated using a Ag-24 wt pct Cu foil interlayer at 800 °C. The results are shown in Figure 8 by the solid line. In this case, the interlayer composition is the same as the liquidus composition at T_b and there is not expected to be any base metal dissolution. Since the temperature has not changed, the interface rate constant should be the same as the original condition, which was $\xi = -0.126$ μm/$\sqrt{s}$. The results give a measured ξ of -0.128 μm/$\sqrt{s}$, which is very close to the results for the eutectic interlayer. The DSC method consistently produces accurate results.

The isothermal solidification kinetics for the Ag-10 pct Cu interlayer are given in Figure 9. The isothermal hold temperature, T_b, was 880 °C, at which temperature the liquidus composition is 10 pct Cu, the same as the interlayer. Thus, as in case of the 24 pct Cu interlayer, there will be no base metal dissolution upon heating to the bonding temperature. The interface rate constant for isothermal solidification as measured from the results in Figure 9 is $\xi' = -0.452$ μm/$\sqrt{s}$. The interface velocity is significantly higher for the 10 pct Cu interlayer held at 880 °C than for the diffusion couples conducted at 800 °C. Assuming that the partition coefficient is constant for all temperatures, the change in the interface rate constant is due solely to an increase in diffusivity according to Eq. [13]. This result is

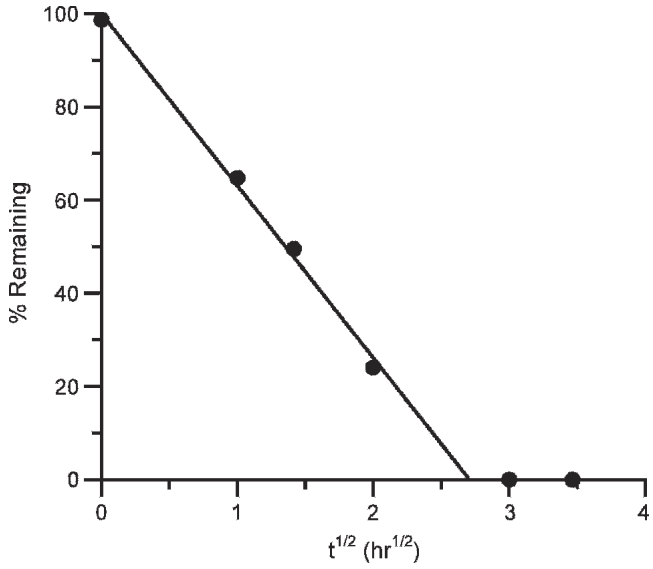

Fig. 8—Fraction of liquid remaining in TLP half-sample after isothermal hold time. The Ag base metal with 24 pct-Cu interlayer bonded at 800 °C.

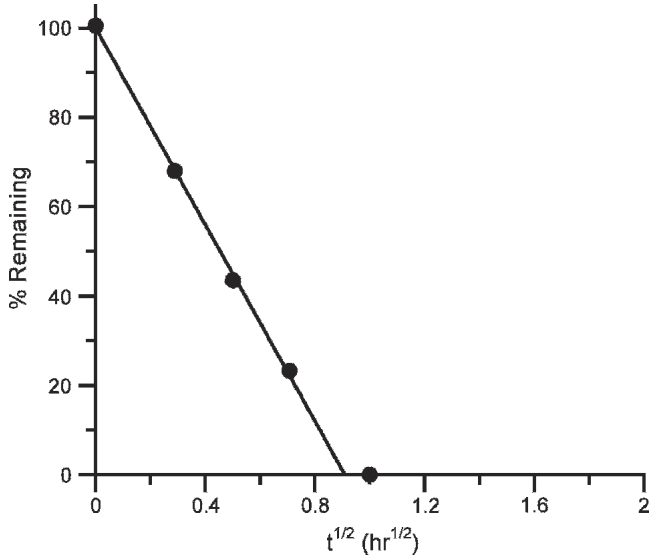

Fig. 9—Fraction of liquid remaining in TLP half-sample after isothermal hold time. The Ag base metal with 10 pct-Cu interlayer bonded at 880 °C.

intuitive since the diffusivity is expected to increase with increasing temperature. The effective diffusivity for this system is found to be $D_{\text{eff}} = 6.4 \times 10^{-9}$ cm^2/s based on the kinetic measurements. This is an entire order of magnitude higher than the effective diffusivity found for the diffusion couples held at 800 °C, which is not unreasonable given the increase in T_b from 800 °C to 880 °C; however, the value is higher than expected using the available diffusion data. Once again, caution must be exercised in using diffusion data that was collected under different conditions than the application.

If Cu is substituted for the base metal using a Ag-Cu eutectic interlayer and an 800 °C isothermal hold temperature, the resulting isothermal solidification kinetics are shown in Figure 10. The resulting interface kinetics give

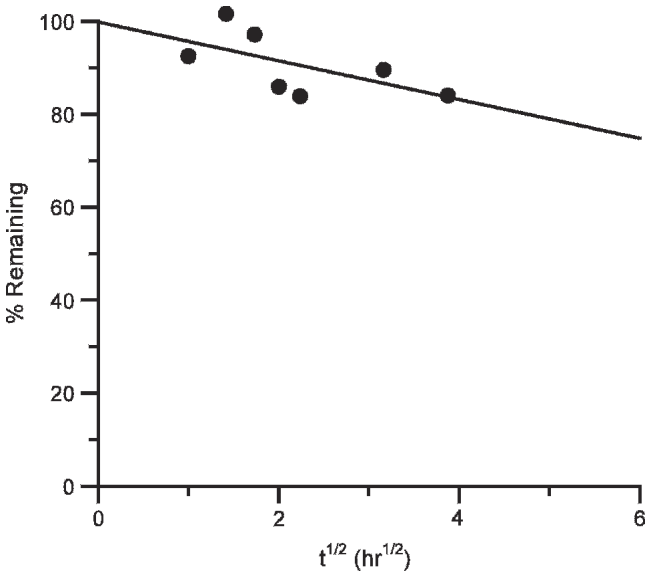

Fig. 10—Fraction of liquid remaining in TLP half-sample after isothermal hold time. The Cu base metal with 25-μm-thick eutectic Ag-Cu interlayer bonded at 800 °C.

an interface rate constant of $\xi' = -0.019\ \mu\text{m}/\sqrt{\text{s}}$ and an effective diffusivity of $D_{\text{eff}} = 3.3 \times 10^{-10}$ cm^2/s. The interface kinetics with the Cu base metal and eutectic interlayer are significantly lower than that measured with the Ag base metal. This is due in part to the lower effective diffusivity, but more to the significantly higher partition coefficient (*i.e.*, 11.1 compared to 2.4) at the Cu-rich end of the phase diagram. It is obvious why this experiment was not carried out to completion since the predicted time required for completion of isothermal solidification is 574 hours.

The results in Figure 10 are compared to the isothermal solidification kinetics observed by MacDonald and Eagar[10] in Table III. The Cu-base metal was TLP bonded using a 101-μm-thick eutectic Ag-Cu interlayer at 820 °C. An interface rate constant of $\xi' = -0.056\ \mu\text{m}/\sqrt{\text{s}}$ was found by measuring the eutectic width, although these results were found to be erroneous, due in part to difficulty in determining the liquid width across the entire joint area. MacDonald and Eagar measured the area under composition profiles of Ag in Cu to relate the liquid width to solute diffused and found better agreement with the prediction ($\xi = -0.021\ \mu\text{m}/\sqrt{\text{s}}$, based on $D_{\text{eff}} = 3.1 \times 10^{-10}$ cm^2/s). These results agree well with the DSC results, but this method is not practical because integration of the composition profiles is a tedious process requiring many measurements.

D. *Effect of Grain Boundaries*

It has been widely reported that grain boundaries provide an enhanced solute diffusion path that results in faster diffusion rates and irrigation of the base metal.[2,8,10,36] This effect has been shown to be negligible in the Ag-Cu system at temperatures above 700 °C in a coarse-grained base metal where there are few grain boundaries to enhance diffusion.[32] Furthermore, at temperatures greater than 80 pct of the melting point, the difference between the bulk and grain boundary diffusivities becomes smaller, reducing grain boundary effects. It has been shown through both

Table III. Comparison of Experimental Interface Kinetics Measured using DSC and Traditional Techniques for Cu-Base Metal

Evaluation Technique	T_b (°C)	ξ ($\mu m/\sqrt{s}$)
DSC method	800	−0.019
Visual inspection[10]	820	−0.056
Concentration profile integration[10]	820	−0.021

experimental and numerical work that the effects of grain boundaries on the nature of solid/liquid interface motion are varied. Fine-grained base metal samples show grain boundary grooving and spherical protrusions causing a significant deviation from the planar solid/liquid interface.[10] Coarse-grained substrates show less deviation from the planar morphology.[37] The isothermal solidification time is reduced significantly with fine-grained base metal; the difference in isothermal solidification rates between coarse-grained and single-crystal base metal is negligible.[10,37,38] The increase in interface kinetics with finer grain size has been attributed to enhanced grain boundary diffusion and grain boundary grooving, although support for this theory by numerical modeling has only been qualitative to date. On the other hand, for coarse-grained substrates bonded at higher temperatures and longer isothermal hold times, it has been shown that the effect of grain boundaries on solid/liquid interface motion is much less significant and can be considered with an effective diffusivity if required.[10,36,39]

Zhou *et al.*[2] point out that the interface kinetics during the isothermal solidification stage can be estimated using an analytical solution as long as the effects of grain boundaries can be neglected. When the grain size is large, the bonding temperature approaches the base metal melting point, and the isothermal hold time is long, the effect of grain boundaries on the process kinetics is minimized, and the analytical solution can be applied. In this study, the process kinetics of isothermal solidification as measured using DSC have been accurately predicted using an analytical solution with published diffusion data. Any grain boundary effects are fully included in the assumed diffusivity.

E. *Metallurgical Analysis*

A cross section of a TLP half-sample shows a eutectic region, a two-phase region, and the single-phase base metal (Figure 11). The eutectic region (dark) is clearly shown in the backscatter electron image in Figure 12. The interface between the eutectic and the two-phase region is scalloped with a cusp that penetrates into the two-phase region of the base metal. Previous work has shown that during cooling from the bonding temperature to the eutectic temperature, primary solidification of α-phase occurs epitaxially at the solid/liquid interface.[19] The scalloped eutectic/base metal interface is evidence of a cellular solidification mode; however, the original liquid width (before cooling) is obscured by the precipitate microstructure and cannot be measured. The two-phase region in Figure 11 clearly shows a discontinuous structure known as cellular precipitation,[40] which occurs during cooling. The reaction front, shown in Figure 13, is a migrating grain boundary that facilitates growth of the precipitates by providing a diffusion path for solute partitioning.[40]

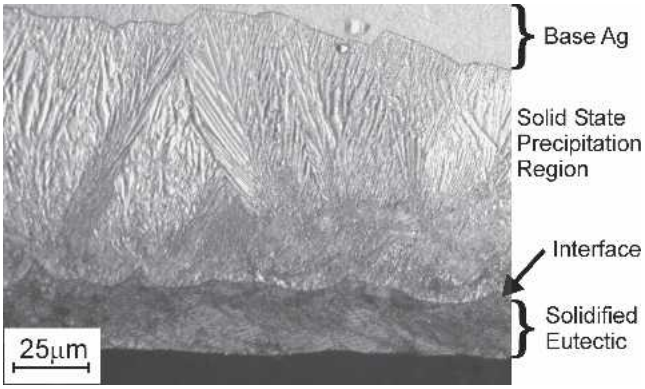

Fig. 11—Interface region of TLP-bonded half-sample after cooling. Three distinct regions are apparent: the solidified eutectic, a two-phase region where cellular precipitation has occurred in the solid state, and the unaffected base metal.[19]

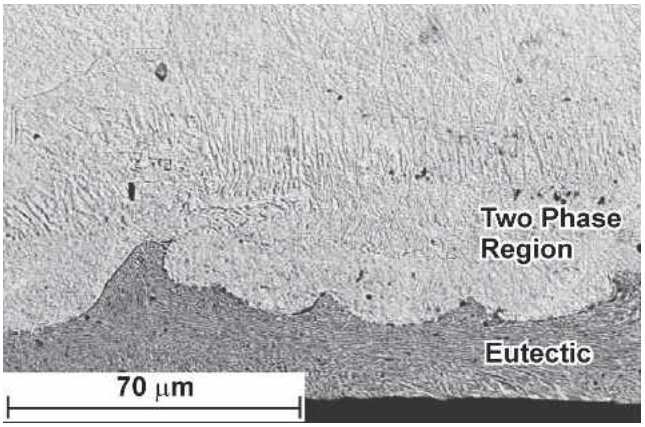

Fig. 12—Backscatter electron image of the interface region showing the eutectic and base metal of a TLP half-sample after cooling.

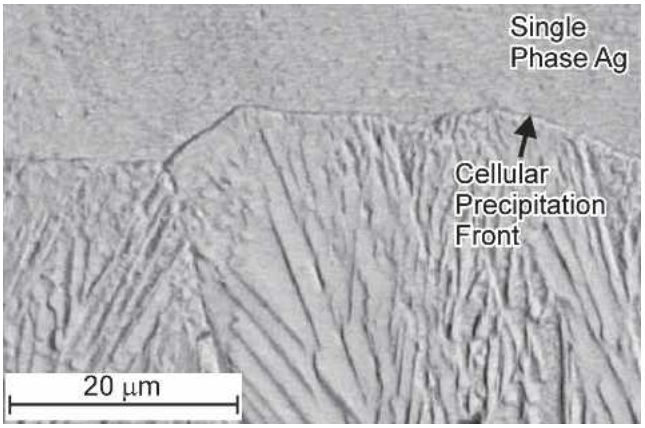

Fig. 13—Solid-state transformation region/base-metal interface showing the migrating cellular precipitation front. Precipitates form upon cooling and obscure the underlying microstructure so primary solidification cannot be observed.

The concentration of Cu was measured at intervals perpendicularly into the base metal from the interface of the eutectic microstructure. To account for primary α-phase solidification, the concentration data has been shifted by some amount to get better agreement with the predicted

profile. The actual distance that the data were shifted depends on the extent of primary solidification and the reference point that was chosen along the eutectic interface. Since this interface was scalloped, there is no uniform distance from the reference point to the original solid/liquid interface. The shifted concentration profiles are shown graphically in Figure 14 and agree well with those predicted by the moving interface model. At shorter distances from the interface, there is significant noise in the measurements caused by the cellular precipitation microstructure. As the distance from the interface increases past the cellular precipitation reaction front, the measured concentration profile becomes smooth and agrees fairly well with the predictions, with points systematically lying slightly above the curve. This could be due to variations in the diffusivity with concentration along the profile. A manual error in shifting the experimental curve for primary solidification will also contribute to the difference.

F. *TLP Full Samples*

The TLP full-sample joints were produced with a 25-μm-thick Ag-28 wt pct Cu foil interlayer. The joints were prepared in a similar manner to the DSC experiment TLP half-samples. The DSC traces of these samples are not of interest since the thick base metal between the joint and the measuring thermocouples dampens heat flow to the point that it cannot be measured. Cross sections of the TLP bonds with increasing isothermal hold times are shown in Figure 15. After 1 hour at the bonding temperature, a uniform layer of eutectic remains at the joint interface. Increasing the hold time to 2 hours results in a thin and broken eutectic layer. The eutectic region is reduced to sparse and irregular pockets after 3 hours and has completely disappeared after 4 hours. Based on the rate constant experimentally measured with the DSC, *i.e.*, $\xi = -0.126\ \mu m/\sqrt{s}$, the expected time required for completion is 3.9 hours. Thus, the rate constant predicted by the DSC shows good agreement with the metallographic results. It would be very difficult to accurately measure the process kinetics using visual inspection to estimate the liquid width, especially if isothermal solidification was not taken to completion. This elucidates that the DSC method provides an accurate quantification of the interface kinetics during isothermal solidification where traditional metallographic techniques have failed.

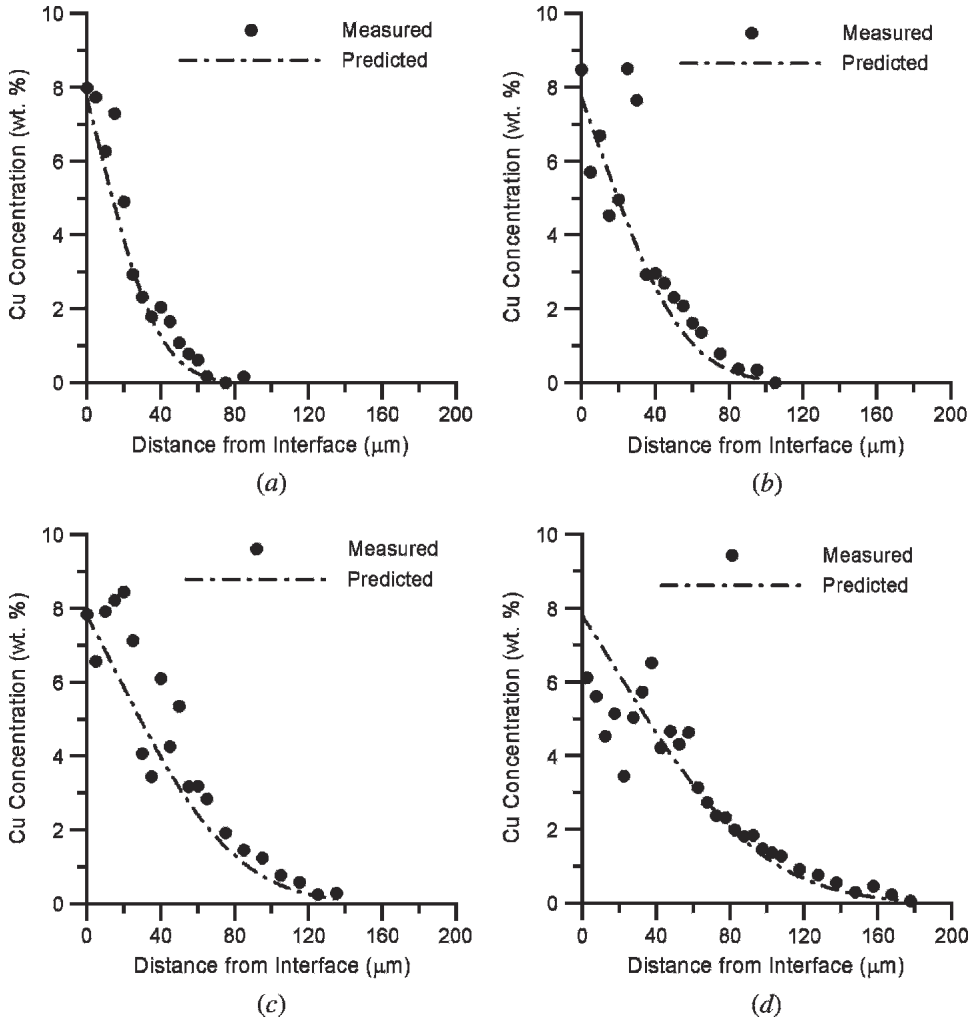

Fig. 14—Cu concentration profiles measured after (*a*) 2 h, (*b*) 4 h, (*c*) 8 h, and (*d*) 12 h. Ag base metal with eutectic Ag-Cu interlayer bonded at 800 °C.

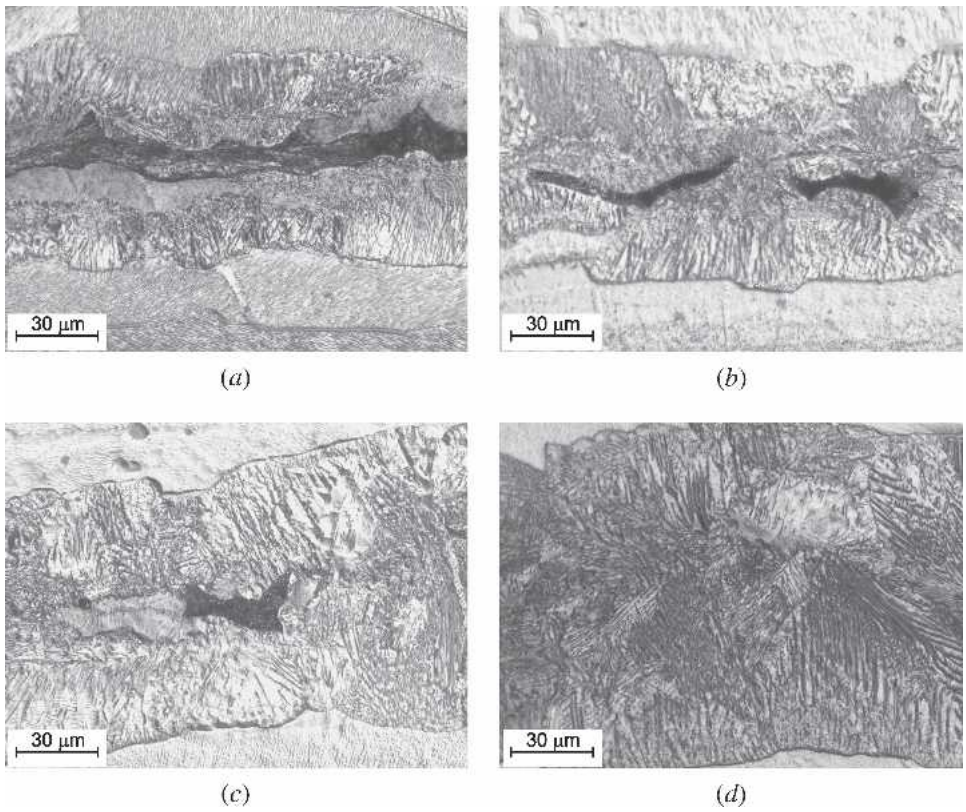

Fig. 15—TLP-bonded samples after (*a*) 1 h, (*b*) 2 h, (*c*) 3 h, and (*d*) 4 h. As expected, the width of the cellular precipitation region increases with time due to increasing penetration of solute in the base metal. The Ag base metal with 25-μm-thick eutectic Ag-Cu interlayer bonded at 800 °C.

V. CONCLUSIONS

A method using DSC to quantify interface motion in a solid/liquid diffusion couple has been used to accurately characterize the process kinetics of the isothermal solidification stage in TLP bonding. The measured interface kinetics are proportional to the square root of the isothermal hold time and can be compared with analytical predictions. Metallographic techniques have been used to validate the DSC results.

1. The measured interface rate constants for the Ag-Cu system with Ag base metal at 800 °C were -0.126 $\mu m/\sqrt{s}$ and -0.128 $\mu m/\sqrt{s}$ for the eutectic and Ag-24 wt pct Cu interlayers, respectively. These values agree well with the interface rate constant predicted by a moving interface solution.
2. The stationary interface solution overestimates the time required for isothermal solidification by a predictable amount. The shifting reference solution systematically underestimates the time for isothermal solidification to reach completion.
3. The accuracy of analytical model predictions is profoundly dependant upon the accuracy of relevant chemical diffusion data. When reliable data are available, the isothermal solidification kinetics given by the moving boundary model are useful in developing TLP bonding process parameters.
4. The interface kinetics measured using the DSC method have been shown to be more accurate than traditional methods, which involve manual estimation of the eutectic width using optical microscopy of metallographic samples. Thus, the DSC method is a valuable tool to be used alongside analytical modeling in the development and refinement of process parameters for TLP bonding.

ACKNOWLEDGMENTS

This study has been supported by Materials and Manufacturing Ontario, an Ontario Centre of Excellence; and the Natural Science and Engineering Research Council.

REFERENCES

1. D.S. Duvall, W.A. Owczarski, and D.F. Paulonis: *Welding J.*, 1974, vol. 53, pp. 203-14.
2. Y. Zhou, W.F. Gale, and T.H. North: *Int. Mater. Rev.*, 1995, vol. 40, pp. 181-96.
3. *Welding Handbook*, 8th ed., L.P. Connor, ed., American Welding Society, Miami, FL, 1989, vol. 1.
4. K. Nishimoto, K. Saida, D. Kim, and Y. Nakao: *Iron Steel Inst. Jpn. Int.*, 1995, vol. 35, pp. 1298-306.
5. M.S. Yeh and T.H. Chuang: *Welding J.*, 1997, vol. 76 (12), pp. 517s-21s.
6. J.P. Jung and C.S. Kang: *Mater. Trans., JIM*, 1996, vol. 37, pp. 1008-13.
7. W.D. MacDonald and T.W. Eagar: in *The Metal Science of Joining*, M.J. Cieslak, J.H. Perepezko, S. Kang, and M.E. Glicksman, eds., TMS, Warrendale, PA, 1992, pp. 93-100.
8. J.E. Ramirez and S. Liu: *Welding J.*, 1992, 71, 10, pp. 365s-75s.
9. H. Ikawa, Y. Nakao, and T. Isai: *Trans. Jpn. Welding Soc.*, 1979, vol. 10, pp. 25-29.

10. W.D. MacDonald and T.W. Eagar: *Metall. Mater. Trans*. A, 1998, vol. 29A, pp. 315-25.
11. Y. Nakao, K. Nishimoto, K. Shinozaki, and C. Kang: *Trans. Jpn. Welding Soc*., 1989, vol. 20, pp. 60-65.
12. T.H. North, K. Ikeuchi, Y. Zhou, and H. Kokawa: in *The Metal Science of Joining*, M.J. Cieslak, J.H. Perepezko, S. Kang, and M.E. Glicksman, eds., TMS, Warrendale, PA, 1992, pp. 83-91.
13. A. Sakamoto, C. Fujiwara, T. Hattori, and S. Sakai: *Welding J*., 1989, vol. 68, pp. 63-71.
14. A. LeBlanc and P. Mevrel: *Proc. Conf. "High Temperature Materials for Power Engineering II,"* E. Bachelet, R. Brunetaud, D. Coutsouradis, P. Esslinger, J. Ewald, I. Kvernes, Y. Lindblom, D.B. Meadowcroft, V. Regis, R.B. Scarlin, K. Schneider, and R. Singer, eds., Dordrecht, The Netherlands, 1990, pp. 1451-60.
15. J.P. Jung and C.S. Kang: *Mater. Trans.*, *JIM*, 1997, vol. 38, pp. 886-91.
16. Y. Nakao, K. Nishimoto, K. Shinozaki, and C.Y. Kang: in *Joining of Advanced Materials*, T.H. North, ed., Chapman and Hall, London, 1990, pp. 129-44.
17. K. Saida, Y. Zhou, and T.H. North: *J. Jpn. Inst. Met*., 1994, vol. 58, pp. 810-18.
18. W.D. MacDonald and T.W. Eagar: *Annu. Rev. Mater. Sci*., 1992, vol. 22, pp. 23-46.
19. M.L. Kuntz, S.F. Corbin, and Y. Zhou: *Acta Mater*., 2005, vol. 53, pp. 3071-82.
20. S.F. Corbin and P. Lucier: *Metall. Mater. Trans*. A, 2001, vol. 32A, pp. 971-78.
21. R. Venkatraman, J.R. Wilcox, and S.R. Cain: *Metall. Mater. Trans. A,* 1997, vol. 28A, pp. 699-706.
22. S.R. Cain, J.R. Wilcox, and R. Venkatraman: *Acta Mater*., 1997, vol. 45, pp. 701-07.
23. J.T. Niemann and R.A. Garrett: *Welding J*., 1974, vol. 53 (4), pp. 175s-84s.
24. H. Nakagawa, C.H. Lee, and T.H. North: *Metall. Trans. A*, 1991, vol. 22A, pp. 543-55.
25. W.F. Gale and D.A. Butts: *Sci. Technol. Weld. Joining*, 2004, vol. 9, pp. 283-300.
26. P.R. Subramanian and J.H. Perepezko: in *ASM Handbook*, vol. 3, *Alloy Phase Diagrams*, H. Baker, ed., ASM INTERNATIONAL, Materials Park, OH, 1992, p. 2.28.
27. I. Tuah-Poku, M. Dollar, and T.B. Massalski: *Metall. Trans. A*, 1988, vol. 19A, pp. 675-86.
28. G. Lesoult: *Center for Joining of Materials Report*, Carnegie Mellon University, Pittsburgh, PA, Sept. 1976.
29. P. Maugis, W.D. Hopfe, J.E. Morral, and J.S. Kirkaldy: *Acta Mater*., 1997, vol. 45, pp. 1941-54.
30. C.W. Sinclair: *J. Phase Equilibrium*, 1999, vol. 20, pp. 361-69.
31. P.V. Dankwerts: *Trans. Faraday Soc.,* 1950, vol. 46, pp. 701-12.
32. J.R. Cahoon and W.V. Youdelis: *AIME Met. Soc. Trans.,* 1967, vol. 239, pp. 127-29.
33. E.A. Brandes: in *Smithells Metals Reference Book*, 6th ed., Butterworth and Co., London, 1983, pp. 13.9-13.54.
34. Y. Zhou: *J. Mater. Sci. Lett.*, 2001, vol. 20, pp. 841-44.
35. Y. Zhou, M.L. Kuntz, and S.F. Corbin: *Proc. Conf. Materials Solutions '02*, ASM International, Materials Park, OH, October 7–9, 2002, 2003, pp. 75-82.
36. Y. Zhou and T.H. North: *Acta. Metall. Mater*., 1994, vol. 42 (3), pp. 1025-29.
37. H. Kokawa, C.H. Lee, and T.H. North: *Metall. Trans. A*, 1991, vol. 22A, pp. 1627-31.
38. K. Saida, Y. Zhou, and T.H. North: *J. Mater. Sci*., 1993, vol. 28, pp. 6427-32.
39. K. Ikeuchi, Y. Zhou, H. Kokawa, and T.H. North: *Metall. Trans. A*, 1992, vol. 23A, pp. 2905-15.
40. D.A. Porter and K.E. Easterling: *Phase Transformations in Metals and Alloys*, 2nd ed., Chapman and Hall, London, pp. 322-26.